Journal of Flow Chemistry (2020) 10:533–543
https://doi.org/10.1007/s41981-020-00092-8

FULL PAPER

On-chip controlled synthesis of polycaprolactone nanoparticles using continuous-flow microfluidic devices

Fazlollah Heshmatnezhad[1] · Ali Reza Solaimany Nazar[1]

Received: 14 November 2019 / Accepted: 24 March 2020 / Published online: 1 April 2020

Abstract

This systematic investigation assessed the potential applications of microfluidic devices in producing a uniform size distribution of polycaprolactone (PCL) nanoparticles by applying the liquid non-solvent precipitation process. Five arrangements of microfluidic devices are fabricated with different designs. The effects of different operational and geometrical factors such as flow rate ratio (FRR), total flow rate (TFR), mixing channel width, mixing channel length, and confluence angles of the inlet channels are investigated on the size, polydispersity index (PDI), and the size distribution of PCL particles. Further, a study was performed to enhance the production throughput of PCL nanoparticles. The mean size of nanoparticles is precisely controlled within the range of 40–370 nm with PDI values of 0.2–0.37. According to the results, the optimal conditions for rapid production of nanoparticles with a size smaller than 200 nm and PDI ≤ 0.31 are obtained at FRR of 8, TFR of 70 ml h^{-1}, channel width of 200 μm, channel length of 20 mm, and the confluence angle of 60°. Furthermore, the microfluidic device with a wider channel width of 600 μm provided a higher productivity rate of the PCL nanoparticles with a similar size and lower PDI than those obtained by other widths.

Keywords Microfluidic device · Hydrodynamic focusing flow · Polycaprolactone nanoparticle · Precipitation process

Introduction

Biodegradable and biocompatible polymeric nanoparticles (NPs) have attracted considerable attention and are widely recognized as successful drug delivery carriers [1–3]. Among the biodegradable polymers, polycaprolactone (PCL) offers a considerable potential for the controlled drug delivery due to its biocompatibility and biodegradability [4].

The size and size distribution of polymeric NPs are the key parameters that play a significant role in the rate of drug release, drug loading, therapeutic efficacy, drug accumulation on specific sites, and the clearance rate of drug from the body [5, 6]. The size of NPs produced should be controlled as it can affect their therapeutic outcomes, which is dictated by production method of carriers [7]. Polymeric NPs are produced via traditional (bulk) methods such as emulsification/solvent evaporation, salting-out, dialysis, nanoprecipitation, and supercritical fluid technology [8]. Among these methods, the nanoprecipitation is a simple and fast method at ambient conditions without utilizing chemical additives or harsh formulation processes [9]. In the nanoprecipitation process, two organic and aqueous phases are required. When the organic phase is slowly injected into a large quantity of the aqueous phase, polymer precipitation occurs immediately after the contact of the two phases [10]. The fluid dynamics in this process should be controlled to produce monodisperse particles. The flow regime or the lateral mixing between two phases strongly affects the nucleation and growth of the particles as well as their aggregation [11].

The NPs synthesized via bulk methods typically suffer from no reproducibility and precise control over the mixing of two phases. These conditions lead to the formation of polydisperse particles in the final products [11]. Thus, microfluidic-based technologies with the ability of overcoming the drawbacks of bulk methods are remarkable in the development of carriers for drug delivery and its discovery [7, 12–16].

Electronic supplementary material The online version of this article (https://doi.org/10.1007/s41981-020-00092-8) contains supplementary material, which is available to authorized users.

✉ Ali Reza Solaimany Nazar
asolaimany@eng.ui.ac.ir

[1] Department of Chemical Engineering, University of Isfahan, Isfahan, Iran

Microfluidics is a branch of engineering which deals with the manipulation of fluids in channels with dimensions less than a millimeter [17–19]. The microfluidic technologies offer a few advantages such as decreasing the reagent consumption, making a faster analysis, offering the ability to enhance the production capacity using parallelization, uniform nanostructural production, better control over process conditions, low energy consumption, and reduced costs [17, 20].

In the previous decade, microfluidic devices were applied to prepare PCL microparticles. Forinstance, Vladisavljevic et al. [21] produced monodispersed microparticles of poly(lactic-acid) (PLA) and PCL utilizing the emulsification method in a flow focusing glass capillary device. They studied the effect of the flow rates of two phases and the geometrical structure of the device on the particle size. They found that the particle size diminished with an increase in the flow rate ratio of continuous phase to dispersed phase. Yang et al. [22] prepared microcapsules of PCL using the microfluidic-emulsification method. They showed that PCL microcapsules can be applied as a smart drug delivery system.

A major issue when using PCL carriers for drug delivery system (DDS) is its particle size which must be within the range of 50–200 nm with a controllable size distribution [23, 24]. These conditions can be achieved by microfluidic hydrodynamic flow-focusing (MHFF) devices accompanied by a non-solvent precipitation process.

In these devices, the production process occurs by introducing an stream containing polymer/organic solvents in the central channel and injecting an aqueous solution into the side channels [17, 25]. The flow regime in MHFF devices is usually defined to low Reynolds number and subsequently the existence of a laminar flow [26]. Accordingly, a well-defined interface (the hydrodynamic focused stream) forms between two phases [27]. The mutual diffusion between the solvent and the water molecules in their interface results in the precipitation of polymer nuclei followed by the formation of NPs. Note that these devices suffer from a limited production throughput [28]. Thus, different designs have been applied to produce more NPs. Most of these designs are complicated, making their application difficult to enhance the production throughput [29–31]. Thus, applying a simple design along with easy fabrication method is more suitable and desirable. Michelon et al. [25] applied several MHFFs with different widths of mixing channel (outlet channel) for liposome production. They found that a wide channel is suitable for a greater productivity of liposomes with similar sizes and lower PDIs than those obtained using narrow widths. Baby et al. [10] also obtained a similar result for PLGA-PEG NPs using MHFF devices. They argued that applying a high range of total flow rate (TFR) in channels with larger dimensions leads to an increase in the production rate. They also studied the effect of mixing channel length on the size of PLGA-PEG particles, and suggested that there were no significant differences between the sizes of the obtained particles at different lengths due to selecting a short range of channel lengths. The channel length is an important parameter as the residence time of fluids can be controlled by utilizing various lengths. Also, achieving a complete mixing depends on the selected range of channel length at high TFR values.

In MHFF devices, the determination of the confluence angle of inlet channels is very crucial to minimize the dynamic perturbations of fluids at the intersection of inlet streams. This is particularly important for the devices that are used to enhance the production throughput as the possibility of flow perturbations increases at high TFRs [32]. Zizzari et al. [33] applied two MHFF devices with confluence inlet angles of 45 and 90° to produce liposome particles. They observed that smaller liposomes were synthesized at a confluence angle of 45°. Previously, the MHFF geometries used to produce polymeric NPs had angles between 45 and 90° in the intersections of inlet channels [3, 9, 10, 34]. In order to clearly recognize the influence of the angle on the size and size distribution of polymeric NPs, two different angles of 60° and 120° were investigated.

To the best of our knowledge, there are only limited studies capturing the effect of different geometrical parameters of MHFF such as width channel and length of mixing channel on polymeric NPs characteristics [10, 25]. Note that one of the most significant factors of MHFF devices is the precise choice of their geometry for achieving an optimum range of NP sizes with increased production rate. Thus, the authors believe that no general, reliable rule has already been offered regarding the effect of MHFF geometries on the size of PCL precipitated particles and its production rate.

Our aim is to examine the nanoparticle production performance of five different designs of MHFF devices for the synthesis of PCL NPs. Thus, a precise study is carried out on the influence of geometrical and operational parameters such as channel width, channel length, confluence inlet angle, flow rate ratio (FRR) of aqueous phase to organic phase, and TFR on the particle size and particle size distribution of PCL NPs. This allows engineering the polymer-based system within the range of 50–200 nm. The production throughput of PCL NPs is also studied. Finally, a comparison is made between the results of the bulk mixing and MHFF methods.

Experimental

Chemicals

Tetrahydrofuran (THF) (HPLC grade, purity ≥99.9%) and PCL (Mw = 14,000 g/mol) were purchased from Sigma-Aldrich, Inc., Germany. Polyvinyl alcohol (PVA, Mw = 13,000–23,000 g/mol, 87–89% hydrolyzed) and Tween 80

as surfactants were also purchased from Sigma-Aldrich, Inc., Germany.

Preparation of organic and aqueous phases

The polymeric solution or the organic phase was prepared by dissolving PCL polymer in the THF solvent at the concentration of 0.3% *w/v*. To prepare the aqueous solution, PVA and Tween 80 surfactants were dissolved in Milli-Q water as non-solvent at 2% w/v and 3.2% w/v concentrations respectively. PVA and Tween 80 surfactants were used together to prevent the agglomeration and coalescence of the produced NPs in the final suspension. Also, it was observed that the simultaneous presence of PVA and Tween 80 prevents the aggregation of particles into microchannels and leads to the formation of a regular focusing flow. Further, PVA and Tween 80 were applied together for further reduction of the size of NPs, compared to using one of them individually. Before being injected, all solutions were passed through 0.22 μm filters (sterile syringe filter, FilterBio, Germany) to remove any particulate impurity.

Fabrication of microfluidic devices

The glass microfluidic devices were fabricated through a standard process of wet-chemical etching and thermal fusion bonding technique. The patterns of the devices' channel were designed using the AutoCAD software. The soda-lime glass substrates were carefully cleaned by distilled water and dried in an oven at 130 °*C* for 20 min. The surfaces were primed with Microposit Primer fumes to improve the photoresist adherence. Then, the glass substrates were coated with a Shipley photoresist (Shipley S1813, Microchem, USA) and baked in an oven at 95 °*C* for 35 min. Next, UV lithography was performed, with the exposed areas developed by immersion in a developer and cleaned by distilled water. Thus, the UV exposed parts of the underlying glass were set open for subsequent etching. The channels were etched using an aqueous solution of 5% buffered hydrofluoric acid during 7 h at 25°*C*. The outlet and inlet connection holes of the channels were manufactured via drilling the micro-slide with carbide drills. The glasses were washed several times with sulfuric acid, ethanol, and ultra-pure water respectively, and dried in an oven at 100 °*C* for 30 min. A flat glass plate was placed on the etched plate. Finally, two glass plates were thermally bonded at 675°*C* for 5 h. The geometrical specifications of these devices are provided in Table 1.

PCL nanoparticle preparation by the microfluidic device

The PCL NPs were produced by the hydrodynamic flow-focusing (HFF) method in a controlled self-assembly process using the liquid non-solvent precipitation (Fig. 1). The microfluidic devices consist of a microchannel with three inlet streams. One stream is the organic phase which flows in the central channel, and two other streams are assigned to the aqueous phase into the branch channels. The two aqueous streams which flow at relatively high flow rates enclose the PCL/THF stream as the focused stream in the central region of the mixing channel, with the precipitation process occurring immediately. Thus, the mutual diffusion of water and THF molecules occurs throughout the focused stream region. In all designs, a desired HFF condition was successfully obtained.

The flow rates of the aqueous phase (Q_{aq}) and organic phase (Q_{or}) were controlled by syringe pump modules (model Borhan MSP-2, Iran) to facilitate the precise control on the formation of focusing stream width and achieve a desired FRR. The FRR was set within the range of 2 to 8 for different designs. The aqueous and organic phases were pumped with 5 ml and 1 ml glass syringes respectively. Poly tetrafluoroethylene (PTFE) tubes (1.2 mm O.D. and 0.6 mm I.D.) and connectors were applied to connect the microfluidic device to the glass syringe. All experiments were performed at room temperature with the HFF stream visualized using an optical microscope (model CZM6, LABOMED, USA). Bright-field micrographs were obtained by a camera (model DigiRetina 500, TUSCEN, China). When the fluids' stream and the formation of the focusing stream became stable upon varying the flow rates of the two phases, the final suspension samples of PCL-assembled structures were collected at the channel output using a glass-flask. Next, the organic solvent of the collected sample evaporated completely in a vacuum oven under reduced absolute pressures. After each experiment, the microchannels were washed and dried.

Characterization of PCL nanoparticles

Size analysis. The size distribution, the mean size (diameter), and PDI of NPs were determined via the dynamic light scattering (DLS) technique using a Vasco particle analyzer (Cordouan Technologies Ltd., Pessac, France) which measures the fluctuations of scattered light as a function of time. All measurements were carried out at 25°*C* utilizing a refractive index of 1.331. The NPs were diluted 3-fold by Milli-Q water before being transferred into the analyzer. The measurement time was 120 s. Each experiment was repeated three times ($n = 3$, mean ± S.D).

The morphology of PCL NPs was observed by Field emission scanning electron microscopy (FESEM) (model Mira 3-Xmu, TESCAN, Czech Republic**)**. The sample was prepared as follows: one drop of NP suspension was poured on a clean mica surface and left to dry at 30°*C*. Then, it was coated with platinum in a Quorum MIRA3 Sputter Coater (Quorum Technologies) and analyzed by an FEI Quanta FESEM.

Table 1 The geometrical specifications of five different microfluidic designs

Design No.	Channel width (μm)	Channel height (μm)	Outlet length (cm)	Confluence inlet angles	Geometry
1	200	200	2	60°	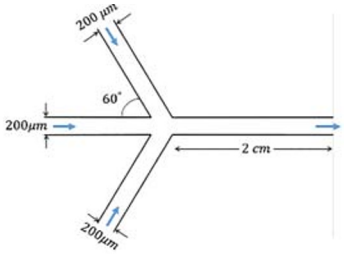
2	300	200	2	60°	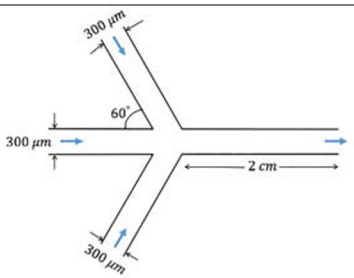
3	600	200	2	60°	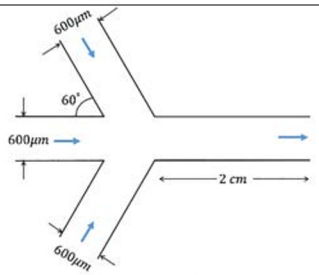
4	300	200	2	120°	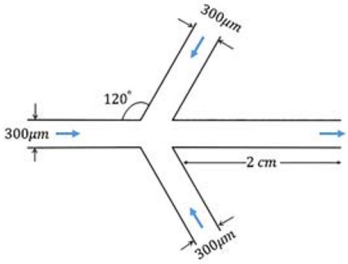
5	300	200	4	120°	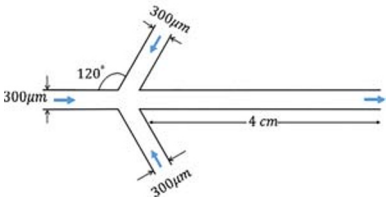

Results and discussion

The effect of the confluence angle with FRR variations on nanoparticle characteristics of PCL

The confluence angle between the central channel and lateral channels is a key parameter that has not been investigated for the synthesis of polymeric NPs in microfluidic devices. For this purpose, two angles of 60° (design 2) and 120° (design 4) were chosen. The mean size and PDI of the produced NPs were reported at a fixed TFR of 40 ml h^{-1} and four different FRRs of 2, 4, 6 and 8. As shown in Fig. 2a, the size of NPs diminished gradually from 157 ± 4.7 to 137 ± 4.6 nm at the FRR of 2 and from 89 ± 3.7 to 71 ± 2.7 at the FRR of 8 upon a decrease in the confluence angle from 120° to 60° respectively. According to the results, a high FRR leads to the production of small particles for both designs. Nevertheless, in the microchannel with a smaller angle, the NPs are smaller as

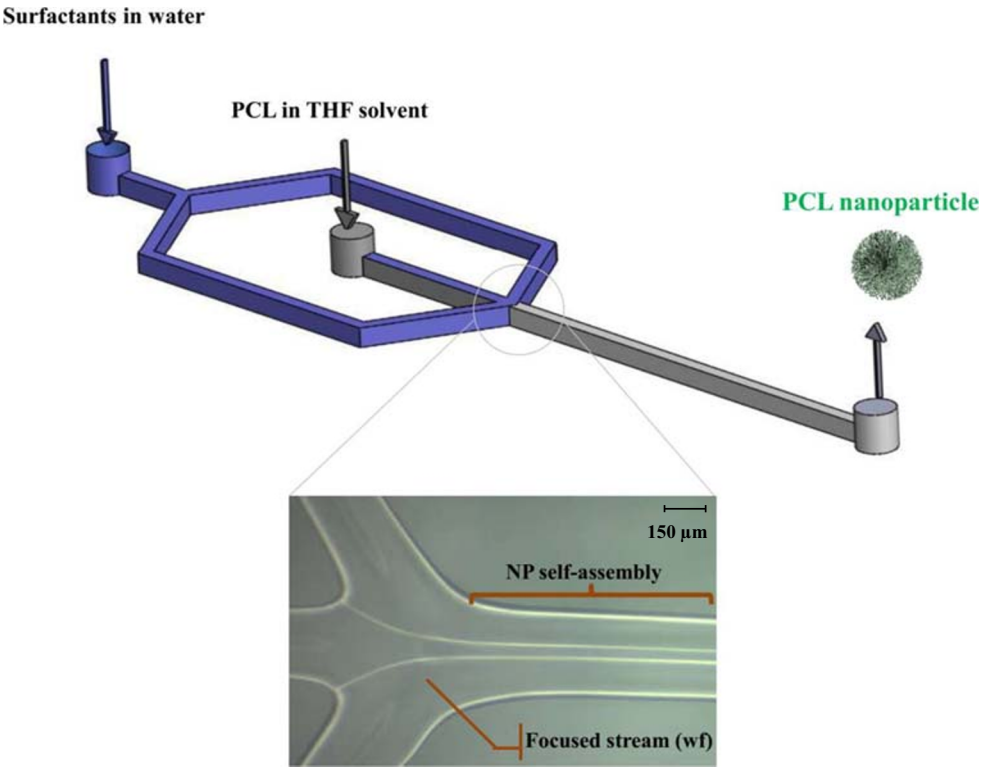

Fig. 1 Sketch of synthesis process of PCL NPs in the MHFF device while observing the focusing stream width (w_f) formed by an optical microscope at FRR of 4 and TFR = 40 ml h^{-1}

compared to the microchannel with a larger angle. At the confluence angle of 60°, an increase in the FRR from 2 to 8 leads to a gradual reduction in the size of NPs and reflects a more mutual diffusion of the THF/water molecules along the mixing channel. On the other hand, at the confluence angle of 120o for the FRRs of 2 to 6, even a three-time increase did not lead to a significant decline in the size of PCL NPs. In both designs, the size of synthesized NPs increased within the FRR range from 8 to 12 (data not shown). Further, for FRR beyond 12, the formation of HFF stream became unstable. Based on the results, the desired FRR ranges between 2 and 8.

Mixing time is an effective parameter which controls the formation process of the particles as well as the final properties and amount of NPs. The mixing performance in MHFF is explained by the diffusive mixing (slow mixing) and convective–diffusive mixing (fast mixing) mechanisms [35]. The convective–diffusive mixing takes place in the region of focusing, while diffusive mixing is induced in the downstream of the mixing channel [35]. At high FRRs (rapid mixing), the particle formation moves toward the convective–diffusive region and reduces the focused stream width whereby the diffusion length to

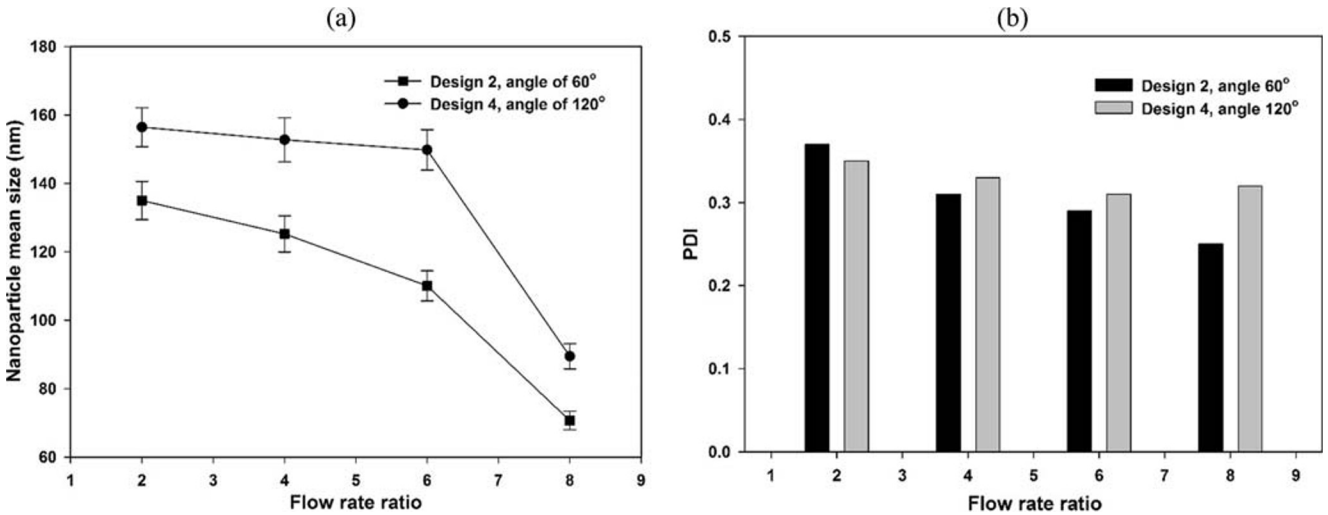

Fig. 2 Effect of confluence angles on (**a**) the size and (**b**) PDI of PCL NPs with the FRR values variations at TFR of 40 ml h^{-1}

achieve a rapid mixing is reduced. Thus, a fall in the particle size and their PDI is observed.

The FRR effect on NPs size can also be explained via the theory of nucleation. The rate of nucleation strongly depends on the supersaturation level which is influenced by the mixing rate of two phases. A rapid mixing at high FRR results in a high supersaturation gradient whereby spontaneous nucleation and small nuclei formation occur. This condition permits production of small polymeric nucleation sites which aggregate to form uniform NPs.

The flow regime within the MHF devices is recognized as laminar (Re < 100) [35]. In these conditions, the residence time of the fluids in the microchannel is crucial. Indeed, the residence time can be expressed as the maximum mixing time required for the formation of NPs. In the device with a confluence angle of 120°, direct collision of streams at the convergent junction site of three inlets leads to the appearance of free vortices. The vortices arise from the inertial forces of the side streams (higher than central stream flow rate) acting on the central stream. Thus, these conditions cause the initial nucleation to occur much earlier than the confluence angle of 60° at a constant length. This, in turn, results in a further growth of the particles, and subsequently the particle size grows. This suggests that fluids have a larger residence time in the mixing channel. Thus, based on the obtained results, for studying the productivity rate at high TFRs, the confluence angle of 60° is desirable due to minimizing the perturbations of streams at the intersection of inlet streams.

According to Fig. 2b, in both designs, the PDIs of the NPs are all under 0.37 at different FRRs, suggesting a homogeneous population of the particles. However, this is followed by an increase in the FRR from 2 to 8to improve the size distribution (Fig. S1) and the formation of monodispersed NPs in the design with confluence angle 60° due to a more uniform nucleation. This supports previous findings in the literature [3, 29, 36–40].

Effect of TFR on nanoparticle characteristics of PCL

The influence of TFR on the self-assembly of PCL NPs is studied using design 2 (Fig. 3). The TFR changes from 24 to 70 ml h^{-1} at different FRRs of 2, 4, and 6. As illustrated in Fig. 3, an increase in the TFR from 24 to 70 mL h^{-1} leads to a decline in the size of the synthesized NPs from 90 ± 9.92 to 91 ± 3.96 nm, and from 118 ± 5.52 to 41 ± 2 nm at the FRRs of 2 and 6 respectively. Othman et al. [36] and Yang et al. [22] examined the effect of TFR on the size of PCL particles and achieved similar results.

The total flow rate determines the residence time inside the microfluidic device through average flow velocity [41]. It is directly proportional to the average flow velocity which is inversely proportional to the residence time. The residence time for different TFRs varied from 240 to 740 ms with the time required for the complete mixing of the streams in design 2 calculated as 182.2 ms by Eq. S3. Thus, the residence time is sufficient for a complete mixing and a homogeneous exchange of solvents, and then the formation of NPs. These conditions justify the effect of TFR on the particle size distribution. In addition, upon increasing TFR, the collision rate of two streams increases due to the effects of shear force on the interfaces of both phases, thereby providing a strong mixing which results in the assembly of small PCL NPs. Further, the shear rate as an efficient factor in the self-assembly dynamics of the PCL NPs leads to the formation of a spherical-shape structure.

However, at TFR >70 ml h^{-1}, no focusing flow is formed and backflow is observed at the inlet intersection. Thus, no controlled synthesis of the NPs occurred in the microfluidic device.

The obtained results reveal that MHFF can operate at higher TFRs, which certainly increases the production throughput along with the production of NPs with the same size characteristics. The PDI values of the synthesized NPs within the range of 0.3 to 0.37 are demonstrated in Fig. 3b at different TFRs and FRRs.

The effect of channel length on nanoparticle characteristics of PCL

The outlet channel length is an important parameter which has not received enough attention in polymeric NP production, whilst it can directly affect the size of PCL NPs. The effects of channel length in the HFF region on the size of NPs and their PDI are studied using designs 4 and 5. Figure 4 indicates that a microchannel with a shorter length—20 mm—produces particles with a smaller size for different FRRs. Since the design 4 with a shorter channel length has a residence time less than that of design 5 (channel length of 40 mm), a a better control is achieved over the synthesis process.

Note the diffusion-driven mixing process is the same for both devices, as mutual exchange/diffusion between two phases occurs at their interface, whose width does not change along the outlet channel. Under this condition, the nucleation and particle growth mechanisms occur competitively. At the beginning of the outlet channel, the nucleation is maximum, as there is a high supersaturation. However, along the channel length, due to the formation of solid phase and then supersaturation reduction, the nucleation is reduced and subsequently the formed primary nuclei grow up to the end of the channel. Thus, given the longer residence time of the particles in design 5, they have more chance for growth and aggregation. Evidently, an increase occurred in the PCL particle size.

Thus, our finding emphasizes that the length of the mixing channel is an effective parameter which can significantly affect the mean size and size distribution of NPs.

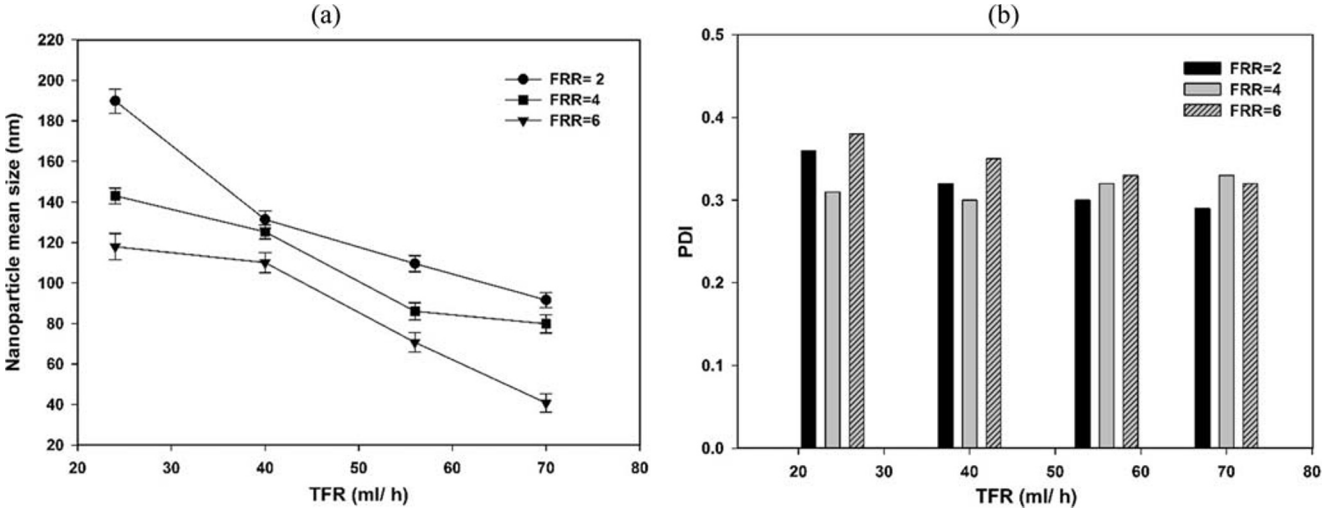

Fig. 3 (**a**) The variation of the particle size and (**b**) PDI with the variations of TFR and FRR in design 2 (channel width of 300 μm,channel length of 20 *mm*)

Low PDIs, ranging between 0.25 and 0.37, are observed for both designs (Fig. 4b). A narrow particle size distribution is obtained for design 4 at the FRRs of 2 and 8, due to the short residence time of nanoparticles at a shorter mixing channel length. However, the effect of FRR variation on the size distribution is more significant at longer channel lengths (Fig. S2).

The effect of channel width on nanoparticle characteristics of PCL

By selecting the confluence angle of 60° as the desired angle between inlet channels, the variations of channel width and subsequently the study of the productivity rate at this angle have been performed for three different designs 1, 2, and 3.

In order to ensure a short diffusion distance (or narrow w_f), microfluidic devices with different outlet channel widths of 200, 300, and 600 μm were chosen. The mean size and PDI of PCL NPs produced in these designs are shown in Fig. 5, at a TFR of 40 ml h^{-1} and the FRR of 2 to 8. According to Fig. 5, as the outlet channel width diminished, a smaller size of NPs was obtained at the same FRR due to a reduction in the width of the focused stream. Thus, the time required for a complete mixing between solvent and non-solvent (Eq.S3) and diffusion length decreased. The mixing time, 49 ms, was lower than the residence time of 77 ms, considering an average velocity of 0.26 m/s. Compared to design 1, applying design 3 (with a wider channel width, 600 μm) led to an increase in the size of NPs; however, the mean size of the particles remained almost at around 200 nm, which is within the optimal range of drug delivery systems [10].

Figure 5b depicts low PDIs of the product within a range of 0.25 to 0.37 for different channel widths at FRRs of 2 and 8. The results show that all of NPs are monodispersed, which is critical for their actual applications. However, the PDI values in design 3 are less than the PDI of two other designs upon

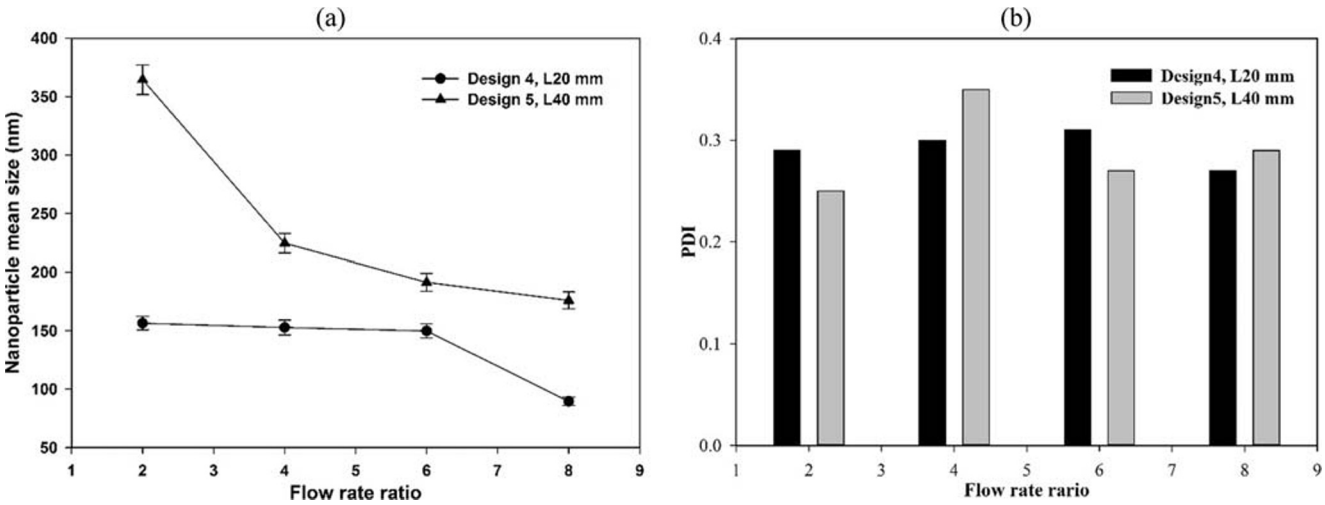

Fig. 4 (**a**) Mean size and (**b**) PDI of PCL NPs as a function of outlet channel length of 20, 40 mm and FRR of 2 to 8 at TFR of 40 ml h^{-1}

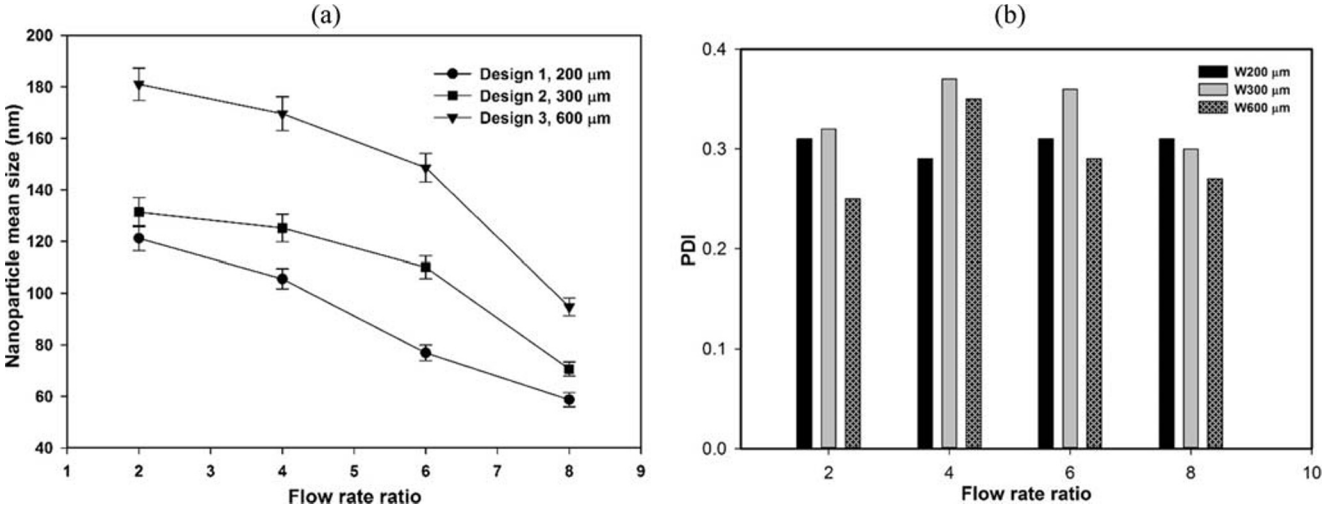

Fig. 5 (**a**) Mean size and (**b**) PDI of PCL NP as functions of channel widths 200, 300, and 600 μm and FRR of 2 to 8 at a TFR of 40 ml h^{-1}

FRR variations. It can be described according to the flow velocity profile. Most probably, as the microchannel width increases, the influence of the non-slip boundary condition diminishes, causing zero velocity in the channel walls. Thus, a uniform distribution of the flow velocity is acquired throughout the mixing region. Michelon et al. [25] confirmed that a wider width of the microchannel resulted in a more uniform fluid velocity profile across the focusing region, thus enabling the production of liposome NPs with a low PDI. Hence, the generation of PCL NPs with a narrow particle distribution can be obtained with adequate selection of FRR and channel width (Fig. S3).

The variations in the mean size of NPs as a function of the width of focused stream are shown in Fig. S4 for designs 1, 2, and 3 with the channel widths of 200, 300, and 600 μm respectively. A wider channel leads to a wider focused stream and an increase in the mixing time at the same FRR. The mean size of NPs can be up to three times wider in the channel width of 600 μm than 200 μm. For the three designs, a good linear relationship is observed between the mean size and width of the focused stream with R^2 values higher than 0.99. It is clear that PCL particle size can be tuned by selecting a suitable FRR value, which is a key parameter in determining w_f. Thus, the width of the focused stream is an indirect measure for determining and tuning the size of PCL NPs.

Influence of the mixing type on nanoparticle characteristics of PCL

In order to identify the dependence of the NP size on the production method, NPs are also synthesized using batch method (S1) and the three mixing types of the two phases are employed: (a) The organic phase is injected by a glass syringe into the aqueous phase under continuous stirring at the solvent/non-solvent volume ratio of 1:4; (b) the aqueous and organic solution streams are pumped using syringe pumps with the flow rates of 8 and 32 ml h^{-1} respectively; (c) the organic phase is pumped using a syringe pump into the aqueous phase under continuous stirring at the solvent/non-solvent volume ratio of 1:4; (d) mixing by the microfluidic device (design 2), where the flow rates are similar to (b). According to Fig. 6a, the NPs formed by the bulk mixing methods show larger sizes ranging from 280 ± 13.8 to 421 ± 23.14 nm, than those produced through design 2 with the size of 125 ± 5.3 nm. Furthermore, the PDI for the microfluidic NPs is remarkably lower (0.3) than the particles prepared by the bulk method with PDI values of 0.36 to 0.57. The high PDIs acquired by the bulk samples are due to broad distributions of the residence time of particles arising from non-uniform mixing causing increased the structural heterogeneity of NPs. In return, a significant increase in the uniformity of the NPs obtained by microfluidic device is attributed to the controlled removal of the THF in a precise fashion. Also, NPs assembly in microfluidic device is reproducible and independent of the user presence, along with an integrated and continuous mixing which is provided through hydrodynamic focused region.

Thus, the mixing nature is very important and the size uniformity of the dispersed systems is a significant feature for pharmaceutical formulations to assure batch-to-batch reproducibility and uniform drug release profiles [42]. Thus, our finding reveals that the microfluidic production of PCL NPs is an appropriate method for medical applications.

The FESEM images of PCL NPs produced by the bulk method (type (c)), designs 2, and 4, are shown in Fig. 6 (B), (C), and (D) respectively at the same FRR and a fixed TFR of 40 ml h^{-1}. The results of bulk method reveal that the NPs have a rough morphology and an asymmetric spherical shape, while the PCL NPs produced using designs 2, 4 have perfect spherical shapes and smooth surfaces during a controlled formation process. Nevertheless, design 4 produces NPs with less regular spherical shapes and a larger size compared to

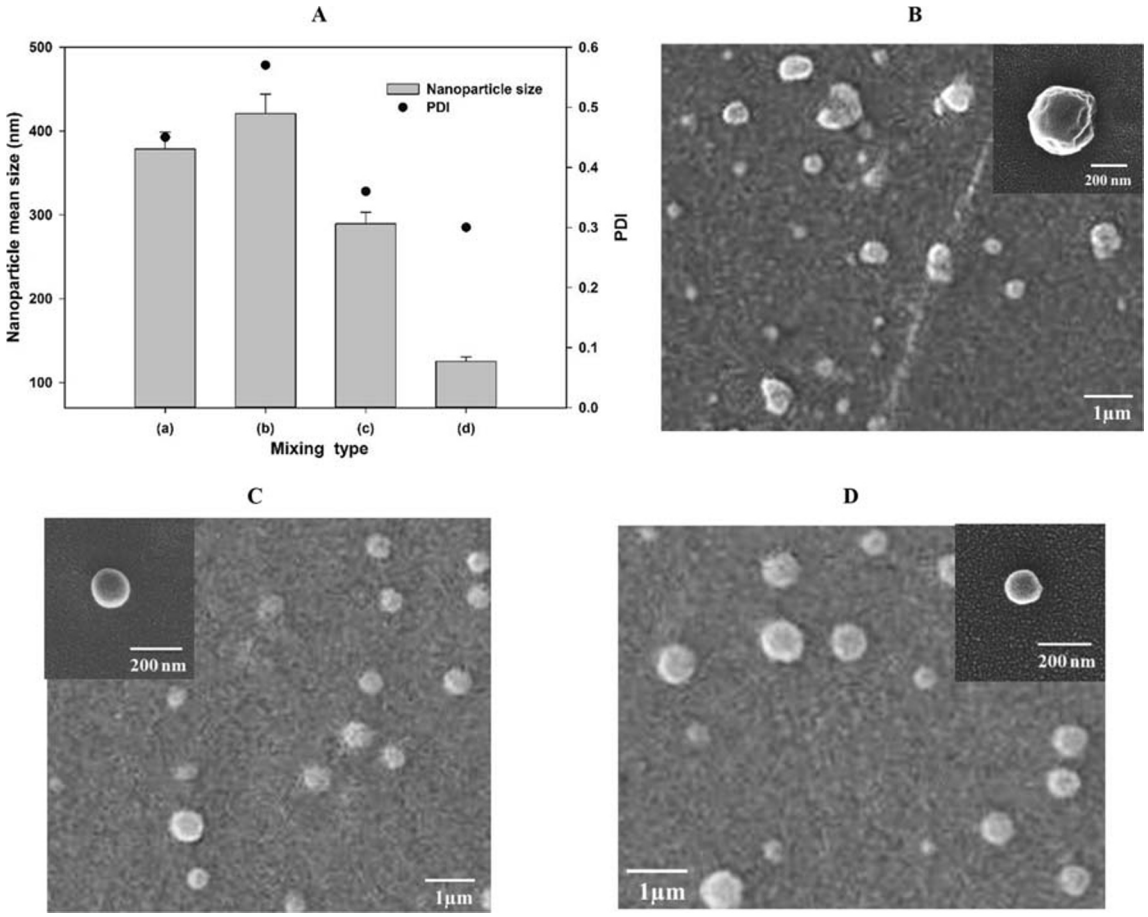

Fig. 6 (**a**) The variations of the particle size and PDI in four types of mixing methods: (**a**) mixing of PCL/THF through injection in the aqueous phase, (**b**) mixing of PCL/THF and aqueous streams, each being pumped using syringe pumps, (**c**) injection of PCL-THF by a syringe pump in the aqueous phase, and (**d**) mixing by the microfluidic device (design 2). (**b**) FESEM images of PCL NPs synthesized using bulk method (types (c)), (**c**) design 2, microchannel with angle 60°, (**d**) design 4, and microchannel with angle 120°

design 2. It can be explained that in the MHF device, the mixing time and residence time are short (order ms). Thus, there is no excessive growth for the formed particles. Furthermore, the movement rate of soluble molecules to the nucleus surface is almost the same in all directions, whereby the particles become spherical in shape to minimize their surface energy and maintain a more stable state. However, in the bulk method, it is not possible to separate the nanoparticles' nucleation from their growth mechanism as there is no precise control over the mixing conditions [43]. Thus, this condition can lead to excessive particle growth which affects the size and shape of the formed particles [43, 44]. Note that the FESEM results are in a good agreement with the results exhibited by the DLS technique, suggesting that the size of PCL NPs in the bulk method is larger compared to both designs.

Scaling-up effect on the particle mean size and calculation of production rate

As mentioned in the previous section, a decline in the outlet width of microfluidic devices successfully produces smaller NPs. Nevertheless, the low production value leads to a very low production yield, which makes this method undesirable for large-scale applications.

A number of strategies could be adopted to enhance the production rate of PCL NPs for industrial applications. Initially, the initial concentration of PCL or TFR should be elevated, and secondly the outlet channel width and the FRR should be adjusted. Accordingly, the PCL NPs were synthesized by applying designs 1, 2 and 3 in order to compare the scale-up effect on the NPs size and their PDI. For this purpose, at the same average flow velocity of 0.5 m s^{-1}, the TFRs were considered at 36, 54, and 108 ml h^{-1} for designs 1, 2, and 3 respectively. Hence, the production rate can be indicated via the following equation [31]:

$$P = \frac{Q_T\, C_p}{1 + FRR} \tag{1}$$

where, $P(mg/h)$, Q_T $(=Q_{aq} + Q_{or})(ml/h)$, and C_p (mg/ml) are the production rate, total flow rate, and the polymer concentration in the THF solvent, respectively.

The production rate grows as the channel width of the microfluidic device increases at the same FRR of 8. Furthermore, it is observed that the production rate increases ~3 times, while the NP size reveals a slight variation among 88 ± 5.9, 108 ± 4.8, and 162 ± 3.6 nm as the channel width grows. The calculated production rate is 13.2 mg h^{-1} for design 1, while it is 19.8 mg h^{-1} for design 2. The production rate could be further improved to 39.55 mg h^{-1} for design 3.

The PDI of 0.28 in the microchannel width of 600 μm is lower than the PDIs of 0.34 and 0.32 in the channel widths of 200 and 300 μm, respectively. These observations are in agreement with the investigation reported by Michelon et al. [25] for liposome formation. Thus, the PCL NPs can be achieved with a narrow distribution through enhancing TFR and using a wider channel width.

These results indicate that the channel width of microfluidic devices has an important technological outcome for industrial applications. In addition, wider microchannels are easier to manufacture and operate than microchannels with a smaller width because of clogging and issues related to increased pressure drop.

Conclusion

For preparing biodegradable polycaprolactone nanoparticles (PCL NPs), a microfluidic platform was developed based on the nanoprecipitation process in 2D microfluidic hydrodynamic flow-focusing (MHFF) devices. The mean size of the NPs was precisely tuned by varying the flow rate ratio (FRR), total flow rate (TFR), outlet channel width, outlet channel length, and channels' confluence angle in different designs of microfluidic devices for achieving the optimal range of the nanoparticles size for drug delivery systems (50–200 nm).

An increase in FRR and TFR resulted in the production of tiny particles. The microchannel with smaller width was able to synthesize smaller NPs as the focused stream width diminished. According to the results, in the microchannel with a shorter length, 20 mm, smaller NPs were produced due to the short residence time of the particles in the mixing channel. A reasonable relationship was observed between the mean size of NPs and the confluence angle, with a small confluence angle of 60^{o} being more favorable for producing smaller NPs. The NPs produced by the bulk method showed a larger size and polydispersity index (PDI) than the NPs obtained from the MHFF device, which was also confirmed by the FESEM results. A microfluidic device with a wider width, 600 μm, and a higher TFR, 108 ml h^{-1}, could be applied for enhancing the production throughput of NPs with a fine size and low PDI. The versatility of microfluidic devices is promising and they can be employed for industrial applications, with a possible advantage of minimizing the degree of microfluidic parallelization. Microchannel designs coupled with facile fabrication method could be applied for the synthesis of polymeric NPs in nanomedical fields and cancer studies.

Acknowledgements The study was financially supported by grant number: 960305 of the biotechnology development council of the Islamic Republic of Iran.

References

1. Kamaraj N, Rajaguru PY, kumar Issac P, Sundaresan S (2017) Fabrication, characterization, in vitro drug release and glucose uptake activity of 14-deoxy, 11, 12-didehydroandrographolide loaded polycaprolactone nanoparticles. Asian J Pharm Sci 12:353–362
2. Jain S, Hirst DG, O'Sullivan JM (2012) Gold nanoparticles as novel agents for cancer therapy. Br J Radiol 85:101–113
3. Capretto L, Cheng W, Carugo D et al (2012) Mechanism of co-nanoprecipitation of organic actives and block copolymers in a microfluidic environment. Nanotechnology 23:375602
4. Dash TK, Konkimalla VB (2012) Poly-ε-caprolactone based formulations for drug delivery and tissue engineering: a review. J Control Release 158:15–33
5. Amoyav B, Benny O (2018) Controlled and tunable polymer particles ' production using a single microfluidic device. Appl Nanosci 8:905–914
6. Laouini A, Charcosset C, Fessi H et al (2013) Preparation of liposomes: a novel application of microengineered membranes - investigation of the process parameters and application to the encapsulation of vitamin e. RSC Adv 3:4985–4994
7. Yaghmur A, Ghazal A, Ghazal RB et al (2019) A hydrodynamic flow focusing microfluidic device for the continuous production of Hexosomes based on Docosahexaenoic acid Monoglyceride. Phys Chem Chem Phys 21:13005–13013
8. Rao JP, Geckeler KE (2011) Polymer nanoparticles: preparation techniques and size-control parameters. Progress Polymer Sci (Oxford) 36:887–913
9. Karnik R, Gu F, Basto P et al (2008) Microfluidic platform for controlled synthesis of polymeric nanoparticles. Nano Lett 8: 2906–2912
10. Baby T, Liu Y, Middelberg APJ, Zhao CX (2017) Fundamental studies on throughput capacities of hydrodynamic flow-focusing microfluidics for producing monodisperse polymer nanoparticles. Chem Eng Sci 169:128–139
11. Donno R, Gennari A, Lallana E et al (2017) Nanomanufacturing through microfluidic-assisted nanoprecipitation: advanced analytics and structure-activity relationships. Int J Pharm 534:97–107
12. Jahn A, Reiner JE, Vreeland WN et al (2008) Preparation of nanoparticles by continuous-flow microfluidics. J Nanopart Res 10:925–934
13. Jahn A, Vreeland WN, Devoe DL et al (2007) Microfluidic directed formation of liposomes of controlled size. Langmuir 23:6289–6293
14. Wlodkowic D, Cooper JM (2010) Tumors on chips: oncology meets microfluidics. Curr Opin Chem Biol 14:556–567
15. Xu Q, Hashimoto M, Dang TT et al (2010) Preparation of Monodisperse biodegradable polymer microparticles using a microfluidic flow-focusing device for controlled drug delivery. Nat Inst Health Public Access 5:1575–1581
16. Gutierrez L, Gomez L, Irusta S et al (2011) Comparative study of the synthesis of silica nanoparticles in micromixer–microreactor and batch reactor systems. Chem Eng J 171:674–683

17. Shi H, Nie K, Dong B et al (2018) Recent Progress of microfluidic reactors for biomedical applications. Chem Eng J 361:635–650
18. Heshmatnezhad F, Aghaei H, Solaimany Nazar AR (2017) Parametric study of obstacle geometry effect on mixing performance in a convergent-divergent micromixer with sinusoidal walls. Chem Prod Process Model 12:1–19
19. Li L-L, Li X, Wang H (2017) Microfluidic synthesis of Nanomaterials for biomedical applications. Small Methods 1: 1700140
20. He P, Greenway G, Haswell SJ (2011) Microfluidic synthesis of silica nanoparticles using polyethylenimine polymers. Chem Eng J 167:694–699
21. Vladisavljević GT, Shahmohamadi H, Das DB et al (2014) Glass capillary microfluidics for production of monodispersed poly (dl-lactic acid) and polycaprolactone microparticles: experiments and numerical simulations. J Colloid Interface Sci 418:163–170
22. Yang C-H, Huang K-S, Lin Y-S et al (2009) Microfluidic assisted synthesis of multi-functional polycaprolactone microcapsules: incorporation of CdTe quantum dots, Fe3O4 superparamagnetic nanoparticles and tamoxifen anticancer drugs. Lab Chip 9:961–965
23. Rizvi SAA, Saleh AM (2018) Applications of nanoparticle systems in drug delivery technology. Saudi Pharm J 26:64–70
24. Cooley M, Sarode A, Hoore M et al (2018) Influence of particle size and shape on their margination and wall-adhesion: implications in drug delivery vehicle design across nano-to-micro scale. Nanoscale 10:15350–15364
25. Michelon M, Oliveira DRB, de Figueiredo FG et al (2017) High-throughput continuous production of liposomes using hydrodynamic flow-focusing microfluidic devices. Colloids Surf B: Biointerfaces 156:349–357
26. Marschewski J, Jung S, Ruch P et al (2015) Mixing with herringbone-inspired microstructures: overcoming the diffusion limit in co-laminar microfluidic devices. Lab Chip 15:1923–1933
27. Evers MJW, Kulkarni JA, van der Meel R et al (2018) State of the art Design and rapid mixing production techniques of lipid nanoparticles for nucleic acid delivery. Small Methods 2:1700375
28. Hood RR, DeVoe DL (2015) High throughput continuous flow production of Nanoscale liposomes by microfluidic vertical flow focusing. Small 11:5790–5799
29. Lim JM, Bertrand N, Valencia PM et al (2014) Parallel microfluidic synthesis of size-tunable polymeric nanoparticles using 3D flow focusing towards in vivo study. Nanomedicine 10:401–409
30. Romanowsky MB, Abate AR, Rotem A et al (2012) High throughput production of single core double emulsions in a parallelized microfluidic device. Lab Chip 12:802–807
31. Kang X, Luo C, Wei Q et al (2013) Mass production of highly monodisperse polymeric nanoparticles by parallel flow focusing system. Microfluid Nanofluid 15:337–345
32. Carugo D, Bottaro E, Owen J et al (2016) Liposome production by microfluidics: potential and limiting factors. Sci Rep 6:1–15
33. Zizzari A, Bianco M, Carbone L et al (2017) Continuous-flow production of injectable liposomes via a microfluidic approach. Materials 10:1411
34. Capretto L, Carugo D, Cheng W et al (2011) Continuous-flow production of polymeric micelles in microreactors: experimental and computational analysis. J Colloid Interface Sci 357:243–251
35. Jahn A, Stavis SM, Hong JS et al (2010) Microfluidic mixing and the formation of nanoscale lipid vesicles. ACS Nano 4:2077–2087
36. Othman R, Vladisavljević GT, Nagy ZK (2015) Preparation of biodegradable polymeric nanoparticles for pharmaceutical applications using glass capillary microfluidics. Chem Eng Sci 137:119–130
37. Feng Q, Sun J, Jiang X (2016) Microfluidics-mediated assembly of functional nanoparticles for cancer-related pharmaceutical applications. Nanoscale 8:12430–12443
38. Sun J, Xianyu Y, Li M et al (2013) A microfluidic origami chip for synthesis of functionalized polymeric nanoparticles. Nanoscale 5: 5262–5265
39. Capretto L, Mazzitelli S, Brognara E et al (2012) Mithramycin encapsulated in polymeric micelles by microfluidic technology as novel therapeutic protocol for beta-thalassemia. Int J Nanomedicine 7:307
40. Othman R, Vladisavljević GT, Hemaka Bandulasena HC, Nagy ZK (2015) Production of polymeric nanoparticles by micromixing in a co-flow microfluidic glass capillary device. Chem Eng J 280:316–329
41. Operti MC, Dölen Y, Keulen J et al (2019) Microfluidics-assisted size tuning and biological evaluation of PLGA particles. Pharmaceutics 11:590
42. Alyami H, Dahmash E, Bowen J, Mohammed AR (2017) An investigation into the effects of excipient particle size, blending techniques and processing parameters on the homogeneity and content uniformity of a blend containing low-dose model drug. PLoS One 12:e0178772, 1–e0178772,19
43. Erdem EY (2013) Microfluidic reactors for the controlled synthesis of Monodisperse nanoparticles. (doctoral dissertation), UC Berkeley
44. Boken J, Soni SK, Kumar D (2016) Microfluidic synthesis of nanoparticles and their biosensing applications. Crit Rev Anal Chem 46: 538–561